Korea-Australia Rheology Journal
Vol. 20, No. 4, December 2008 pp. 197-211

A critical review on blood flow in large arteries; relevance to blood rheology, viscosity models, and physiologic conditions

Fuat Yilmaz and Mehmet Yaşar Gundogdu*
University of Gaziantep, Department of Mechanical Engineering, 27310 Gaziantep/TURKEY
(Received February 7, 2008; final revision received May 6, 2008)

Abstract

The purpose of this study is mainly directed towards present of viewpoints on critical and commentary analysis on blood rheology, blood viscosity models, and physiological flow conditions. Understanding these basics is fundamental to meet the need for a sufficient and reliable CFD model of blood. Most of the used viscosity models on this manner have determined from parameter fitting on experimental viscosity data. Availability of experimental data from literature to define viscosity models of CFD analysis should be accurately chosen and treated in order to avoid any errors. Several basic gaps that limit the CFD model results are identified and given opportunities for future research.

Keywords : blood flow, blood rheology, viscosity model, CFD model, viscoelasticity, thixotropy, yield stress

1. Introduction

A critical rate of deaths in developed communities nowadays results from cardiovascular diseases, most of which are associated with unusual hemodynamic conditions in arteries. Understanding of blood flow hemodynamics has great importance in testing the hypothesis of disease formation, assessment and diagnosis of the cardiovascular disease, vascular surgery planning, modeling the transport of drugs through the circulatory systems and determining their local concentrations, predicting the performance of cardiovascular equipments or instruments that have not yet been built such as heart valves, stents, probes, *etc.*, and devising better therapies of mainly coronary artery occluding, atherosclerosis, thromboses, vasculitis or varicose, aneurysms, *etc.*

The arterial blood flow in the human body is typically a multiphase non-Newtonian pulsatile flow in a tapered elastic duct with the terminal side and/or small branches. The pulsatile flow is an unsteady flow in which resultant flow is composed of a mean and a periodically varying time-dependent component. Pulsatile flow is responsible for submissive effect on time-dependent viscoelastic and thixotropy behavior of blood. Pulsatile flows have been investigated as experimentally and theoretically with an increasing rate since the first quarter of 20th century (Gundogdu and Çarpinlioglu, 1999a; Gundogdu and Çarpinlioglu, 1999b; Çarpinlioglu and Gundogdu, 2001). Initial studies were generally carried by mathematicians with analytical methods whereas similar studies have recently conducted densely in medicine and engineering fields. In view of these recent studies, new science fields such as bio-fluid mechanics, bioengineering, and biomedical engineering are therefore rather popular nowadays.

Computational fluid dynamics (CFD) has proven to be a practical, efficient, and reliable tool for investigating blood flow cases due to the advantage of low cost and simplicity of testing different physiological conditions. The performance of CFD models is however directly dependent on blood rheology and the local environment of flow medium such as physiological flow conditions, mechanical properties of blood vessels, interactive forces between blood plasma (liquid phase) and blood cells (solid-like phase), *etc.* The measurement of blood properties under different hemodynamic conditions has therefore gained great importance to obtain proper rheological models for CFD analysis. The studies on blood rheology are initially reviewed in the present study because it is accepted as an Achilles' heel for understanding the present status of blood flow modeling. After that the studies related with blood viscosity models and physiological flow conditions are also successively discussed to clarify the transfer perspective of the gained erudition from the rheological measurements up to blood CFD models. Details of some hemorheological models are available in the papers of Cho and Kensey (1991) and Zhang and Kuang (2000). This review consolidates the whole provision of current knowledge of limitations in availability of experimental data with rheometer, more recent hemorheological models and relevant data.

*Corresponding author: gundogdu@gantep.edu.tr

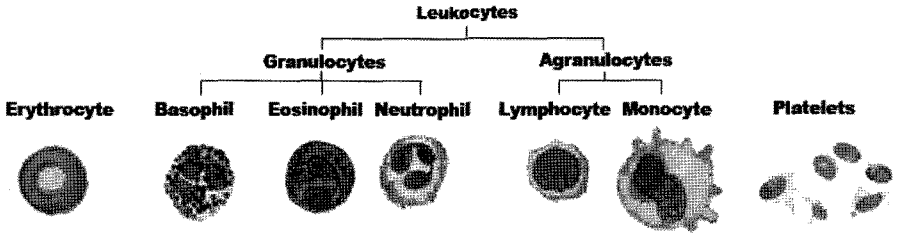

Fig. 1. Types of blood cells.

Table 1. The physical properties of RBCs

	Diameter (μm)	Thickness (μm)	Neck (μm)	Surface Area (μm^2)	Volume (μm^3)	Mass Density (g/cm^2)
Normal Physiologic Range	6-9	1.84-2.84	0.81-1.44	120-163	80-100	1.089-1.100
Typical Value	7.5	-	-	140	90	1.098

2. Blood composition and structure

Blood composition and structure play a vital role in blood rheology. Blood consists of a suspension of elastic particulate cells in a liquid known as plasma. Human blood plasma, the continuous phase of blood, is about 91% water, 7% proteins, 2% inorganic solutes, and other organic substances of its weight (Mazumdar, 1998). Potential non-Newtonian properties of plasma were considerable debate until the early 1960 (Zydney *et al.*, 1991), but recent studies have demonstrated that plasma is a Newtonian fluid with a viscosity of about 1.2 mPa·s at 37°C (Pal, 2003) and its viscosity is a function of temperature (De Gruttola, 2005).

$$\mu_p = \mu_{p=37^\circ C} \exp[0.021(37-T)] \quad (1)$$

The particulate second phase of blood consists of erythrocytes or red blood cells (RBCs), leukocytes or white blood cells (WBCs), and platelets as shown in Fig. 1. RBCs are the predominant cell type of blood and represents cellular volume fraction more than 99% (Picart *et al.*, 1998a). The RBC volume fraction is called as the hematocrit and its normal range is 0.47 ± 0.07 in adult human males and 0.42 ± 0.05 in adult females (Pal, 2003). RBCs have a biconcave discoid shape and their physical properties are given in Table 1 (Bronzino, 2006). They consist of a thin elastic membrane enclosing hemoglobin solution that is a Newtonian fluid with a viscosity of about 6 mPa·s (Snabre and Mills, 1996) and this makes it possible for RBC to deform.

The aggregatable and deformable nature of the red RBCs plays significant roles in blood rheology. RBC aggregation causes a large increase in viscosity at low shear rates. The size of RBC aggregation is a function of RBC concentration and shear rate (Zydney *et al.*, 1991). The existence of aggregation also depends on the presence of fibrinogen and globulin proteins in plasma (Fung, 1993). When shear rate tends to zero, RBCs become one big aggregate, which then behaves like a solid. As the shear rate increases, RBCs aggregates tend to be broken up and the structure becomes a suspension of a cluster of RBCs aggregates in plasma. These aggregates are in turn formed from smaller units called rouleaux as shown in Fig. 2 (Fung, 1993). As the shear rate more increases, the average number of RBCs in

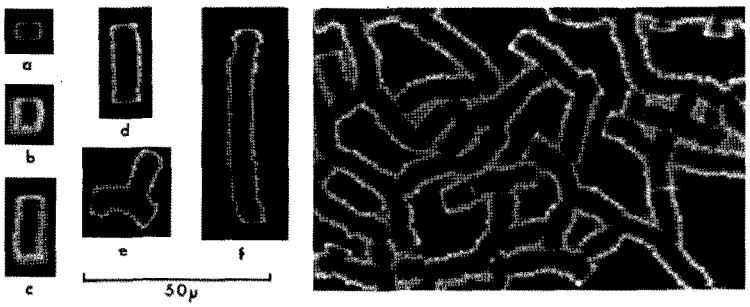

Fig. 2. Rouleaux of human red cells photographed on a microscope slide showing single linear and branched aggregates (left part) and a network (right part). The number of cells in linear array are 2, 4, 9, 15, and 36 in a, b, c, d, f, respectively (Fung, 1993).

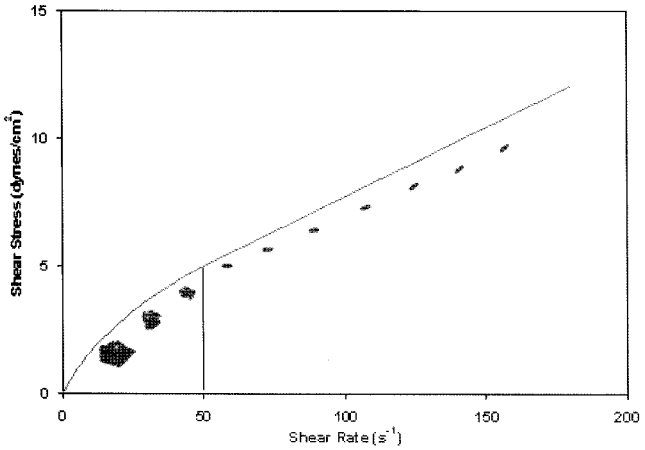

Fig. 3. Dynamic equilibrium between cell aggregate size and shear stress applied (Mazumdar, 1998).

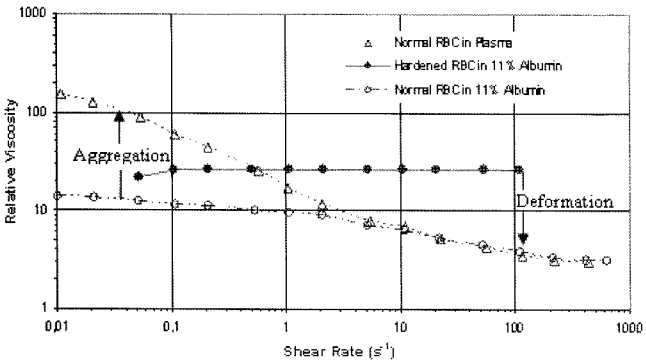

Fig. 4. Logarithmic relations between relative apparent viscosity and shear rate in three types of RBC suspensions, each containing 45% hemotocrit value (Chien, 1970).

each rouleaux decreases. If the shear rate is larger than a certain critical value, the rouleaux are broken up into individual cells. At subcritical shear rates, the RBCs in each rouleaux maintain their rest-state equilibrium shape, biconcave discoid shape. If the shear rate is supercritical, the RBCs are dispersed in plasma separately and tend to become elongated and line up with the streamlines (see Kang (2002) for more details). Dynamic equilibrium between cell aggregate size and applied shear stress is shown in Fig. 3 (Mazumdar, 1998).

Fig. 4 illustrates the mechanisms underlying the non-Newtonian behavior of blood (Chien, 1970). It shows the relationship between relative viscosity and shear rate for three different types of RBCs suspensions namely; RBCs suspended in normal plasma (NP), RBCs suspended in albumin (NA), and hardened RBCs in albumin (HA). The relative viscosity is defined as a ratio of the suspension viscosity to the plasma viscosity. The properties of the RBCs can be altered chemically to isolate certain effects. RBCs were hardened to prevent deformation, and the albumin was used to maintain the normal cell shape. The lack of other proteins in albumin solution prevents the aggregation. In this way, the effect of aggregation and deformation of the RBCs on the blood viscosity were clarified. The difference between the NP and NA curves indicates the effect of cell aggregation, whereas that between NA and HA indicates the effect of cell deformation. Aggregation of red cells at low shear rates leads to increase of viscosity. Red cells elongation and orientation at high shear rates lead to decrease of viscosity further. In addition, the viscosity of the hardened RBC suspension seems independent of shear.

The studies related with RBC behaviors in the microcirculation (Cristini and Kassab, 2005), in the venous (Bishop *et al.*, 2001) and in general (Baskurt and Meiselman, 2003; Rampling *et al.*, 2004; Popel and Johnson, 2005) were recently reviewed. The mechanisms of RBC aggregation are figured out by the balance of aggregation and disaggregation force. Disaggregation forces mainly consist of mechanical shear force, repulsive force, and elastic energy of RBC membrane. However, the mechanism of aggregation force is unclear. As mentioned in the review articles and Baumler *et al.* (1999), the bridging, due to the adsorption of macromolecules onto adjacent cell surfaces, and the depletion, due to the osmotic gradient arising from the exclusion of macromolecules near the cell surface, molecular models are presently used to describe aggregation behaviors. Recently, the aggregation, deformation and dynamic motion of RBCs in shear flow is investigated by hemoreological models capable of modeling the coupled fluid structure interaction. Liu *et al.* (2004) used a two dimensional modeling technique that couples Navier-Stokes equations with using Morse potential to determine the cell aggregation in the framework of the immersed finite element method. Microscopic mechanism of RBC aggregation is connected to the macroscopic behaviors of the blood, such as the shear rate dependence of blood viscosity (Liu and Liu, 2006). Bagchi *et al.* (2005) also simulated the RBC aggregation behaviors by using bridging model and front tracking/immersed boundary method for multiple fluids. Cell to plasma viscosity ratio and the shear modules of the cell membrane determine the level of cell deformability and have a significant role on the stability and motion of the aggregate (Bagchi *et al.*, 2005). Dupin *et al.* (2007) is used lattice Boltzmann method (LBM) and a harmonic spring model to simulate dense suspension of deformable RBCs. RBC deformation is also simulated by Bagchi (2007) with a large ensemble containing about 2500 RBCs. The immersed boundary method to incorporate the fluid membrane interaction has been combined with LBM investigate RBC behaviors considering the RBC membrane mechanics, plasma/cytoplasm viscosity difference, intercellular interaction and the hydrodynamic viscous force (Zhang *et al.*, 2007; Zhang *et al.*, 2008).

It can be easily understand from the studies directed on

the structure of blood that the blood viscosity is dependent on the physiological flow conditions of blood and the blood composition properties such as hematocrit, temperature, shear rate, cell aggregation, cell shape, cell deformation and orientation. All of these observed dependencies should be formulated and then systematically introduced into some blood viscosity models for use in CFD analysis of blood flow. The review of the present viscosity models discussed in the following section however showed that; the effects of cell aggregation, cell shape, cell deformation, and cell orientation have not clearly reflected in the viscosity models, although these models considers the effects of hematocrit or cell concentration, shear rate, and temperature. However, numerical studies on RBC behaviors give a hope for transferring available knowledge of microscopic hemodynamic and hemorheological behaviors to a blood viscosity model.

3. Blood viscosity models

Experimental investigations over many years showed that blood flow exhibits non-Newtonian behavior such as shear thinning, thixotropy, viscoelasticity, and yield stress. Its rheology is influenced by many factors including plasma viscosity (Baskurt and Meiselman, 2003), alignment of RBCs (Baskurt and Meiselman, 1977), level of RBC aggregation and deformability (Chien, 1970), fibrinogen (Chien *et al*, 1970), flow geometry and size (Thurston and Henderson, 2006), rate of shear, hematocrit, male or female, smoker or non-smoker, temperature, lipid loading, hypocaloric diet, cholesterol level, physical fitness index (Cho and Kensey, 1991), diabetes mellitus, arterial hypertension, sepsis (Meiselman and Baskurt, 2006), *etc.* The blood viscosity models in literature may however be discussed in two main categories namely; Newtonian viscosity models and non-Newtonian viscosity models.

3.1. Newtonian viscosity models

The blood behaves like a Newtonian fluid when shear rate over a limiting value. This apparent limiting viscosity or shear rate is a function of the blood composition, and is primarily modulated by hematocrit (Crowley and Pizziconi, 2005). There have been a variation in the literature on this limiting shear rate as that; 50 s^{-1} (Long *et al.*, 2004), 100 s^{-1} (Chan *et al*, 2007) or in the range of 100 to 300 s^{-1} (Crowley and Pizziconi, 2005). Due to the high shear rate in large arterial blood vessels (*i.e.*, vessel diameter $\geq$ 1 mm (Cho and Kensey, 1991)), blood was modeled as a Newtonian fluid in some studies by accepting the viscosity of blood to be constant and equal to the blood viscosity (generally accepted 3.5 mPa·s) corresponding to the high limiting shear rate. However, a considerable amount of attempts has been developed for estimating Newtonian viscosity of whole blood as a function of cell concentration, plasma viscosity, and maximum packing fraction for determining the relative viscosity of dispersed systems as given in Table 2.

As can be seen from Table 2, concentration dependent Newtonian models can be used to determine hematocrit dependence of the zero, μ_o and infinite, μ_∞ shear viscosity of blood. A wide variety of studies on the concentration dependence mainly extends the well-known study of Einstein on monodisperse dilute rigid spheres. In later developments, interactions between particles have been included by adding a quadratic terms in ε, and the particle shape effects have been included by using a shape factor or maximum volume fraction, ε_{max} in the range from approximately 0.5 to 0.75 even for monodisperse spheres (Barnes *et al.*, 1989). Reformed types of Einstein equation have been used for high concentration. The effect of shear induced particle migration was also appended by using the local particle concentration, ε_w (Phillips *et al.*, 1992). Viscosities of dispersed phase, μ_d and continuous phase, μ_c have been included for deformable elastic particles. Some of these models were extended to the non-Newtonian models by taking some model parameters as shear dependent variables (Quemada, 1978; Wildemuth and Williams, 1984; Snabre and Mills, 1996) and by using the differential developing effective medium approach (Pal, 2003).

3.2. Non-Newtonian viscosity models

The instantaneous shear rate over a cardiac cycle varies from zero to approximately 1000 s^{-1} in several large arteries (Cho and Kensey, 1991). Therefore, over a cardiac cycle, there are time periods where the blood exhibits shear thinning behavior. In addition to low shear time periods, low shear exists in some regions such as near bifurcations, graft anastomoses, stenoses, and aneurysms (Leondes, 2000). Blood in those regions appears to have non-Newtonian properties. To model the shear thinning properties of blood, a constitutive equation is necessary to define the relationship between viscosity and shear rate. The various non-Newtonian blood models have been used to relate the shear stress and rate of deformation for the blood flow in large arterial vessels. In addition to shear thinning behavior, thixotropic and elastic behaviors of blood have also been taken into account by various researchers. All of these models can be classified into two categories as time independent and time dependent flow behavior models. The constants of the time independent models were obtained by means of parameter fitting on experimental viscosity data obtained at certain shear rates under steady state conditions (Ai and Vafai, 2005; Ballyk *et al.*, 1994; Braun and Rosen, 2000; Cho and Kensey, 1991; Cosgrove, 2005; Fung, 1993; Johnston *et al.*, 2004; Lee and Steinman, 2007; Luo and Kuang, 1992; Malkin, 1994; Rao, 1999; Rovedo *et al.*, 1991; Schramm, 2005; Steffe, 1996; Zhang and Kuang, 2000; Zydney *et al.*, 1991).

Table 2. Relative viscosity based on concentration dependence of dispersions

$\mu_r = 1+2.5\varepsilon$	(Einstein, 1911)
$\mu_r = 1+2.5\varepsilon+6.2\varepsilon^2$	(Batchelor, 1977)
$\mu_r = 1+2.5\varepsilon+10.05\varepsilon^2+0.00273\exp(16.6\varepsilon)$	(Thomas, 1965)
$\mu_r = (1.4175+5.878\varepsilon-15.98\varepsilon^2+31.964\varepsilon^3)\mu_p$	(Lee and Steinman, 2007)
$\mu_r = [1-(\varepsilon/\varepsilon_{max})]$	(Krieger, 1972)
$\mu_r = [1-(\varepsilon/\varepsilon_{max})]^{-[\eta]\varepsilon_{max}}$	(Krieger and Dougherty, 1959)
$\mu_r = [1-(\varepsilon/\varepsilon_{max})]^{-2}$	(Maron and Pierce, 1956)
$\mu_r = [1-(\varepsilon/p)]^{-2}$	(Kitano *et al.*, 1981)
$\mu_r = [1-0.5p\varepsilon]^{-2}$	(Quemada, 1978)
$\mu_r = [1-(1.25\varepsilon/(1-(\varepsilon/\varepsilon_{max})))]^2$	(Eilers, 1941)
$\mu_r = 9/8((\varepsilon/\varepsilon_{max})^{1/3}/(1-(\varepsilon/\varepsilon_{max})^{1/3}))$	(Frankel and Acrivos, 1967)
$\mu_r = [1+0.75(\varepsilon/\varepsilon_{max})/(1-(\varepsilon/\varepsilon_{max}))]^2$	(Chong *et al.*, 1971)
$\mu_r = \exp[2.5\varepsilon(1-p\varepsilon)]$	(Mooney, 1951)
$\mu_r = \exp(p\varepsilon)$	(Richardson, 1933)
$\mu_r = \exp(p_1\varepsilon+p_2)$	(Broughton and Squires, 1938)
$\mu_r = \exp[(p\varepsilon)/(1-(\varepsilon/\varepsilon_{max}))]$	(Krieger, 1972)
$\mu_r = \exp[(p_1-p_2/\varepsilon_{max})\varepsilon]/(1-(\varepsilon/\varepsilon_{max}))^{p_2}$	(Vocadlo, 1976)
$\mu_r = 1/(1-\varepsilon^{1/3})$	(Hatschek, 1911)
$\mu_r = 1/(1-(p\varepsilon)^{1/3})$	(Sibree, 1931)
$\mu_r = (1-\varepsilon)^{-2.5}$	(Brinkman, 1952; Roscoe, 1952)
$\mu_r = (1+[(\varepsilon/\varepsilon_{\eta_r=100})/(1.187-(\varepsilon/\varepsilon_{\eta_r=100}))])^{2.492}$	(Pal and Rhodes, 1989)
$\mu_r = 1+2.5\varepsilon[([\mu_d/\mu_c]+0.4)/([\mu_d/\mu_c]+1)]$	(Taylor, 1932)
$\mu_r = (1-\varepsilon(([\mu_d/\mu_c]+0.4)/([\mu_d/\mu_c]+1)))^{-2.5}$	(Dintenfass, 1968)
$\mu_r = (1+\varepsilon)/(1+p\varepsilon)$	(Jeffery, 1922)
$\mu_r = exp[4.1\varepsilon/(1.64-\varepsilon)]$	(Vand, 1948)
$\mu_r = (1-(\varepsilon/\varepsilon_{max}))^{-1.82}$ where $\varepsilon = (\varepsilon_w/\bar{r})((1-(\varepsilon_w/\varepsilon_{max}))/(1-(\varepsilon/\varepsilon_{max})))^{1.82(1-K_\eta/K_c)}$	(Phillips *et al.*, 1992)
$\mu_r = (1+\varepsilon(0.5\kappa-1))/((1-\kappa\varepsilon)^2(1-\varepsilon))$	(Toda and Furuse, 2006)
$\mu_r = (1+1.5\varepsilon)/(1-\varepsilon)$	(Lew, 1969)

At this point it should be noted that; many existing viscosity data of whole blood were taken under assumption of Newtonian flow pattern in the rheometer's measurement field and ignored slip effect. In addition to these criteria, some data have been fitted and used with neglecting the effect between physiologic blood temperature and medium temperature of measurement on CFD studies. All of these assumptions can cause to errors. The flow pattern and shear rates of blood in the rheometer are different from a Newtonian fluid. Overestimation of up to 20% in whole

blood apparent viscosity has been observed when the shear rate is assumed to be that for a Newtonian flow pattern (Janzen *et al.*, 2000). Therefore, apparent shear rate and viscosity need to corrections. Some correlation methods for blood or Casson fluid like blood have been used in the literature (Janzen *et al.*, 2000; Joye, 2003; Zhang and Kuang, 2000), but they need to include the effect of hematocrit or void fraction. Since different flow patterns may be observed at different hematocrit values.

The slip effect is a common feature for all types of two-phase or multiphase systems like blood (Barnes, 1995). It is significant only if the slip layer is sufficiently thick or the viscosity of the slip layer is sufficiently low (Coussot, 2005). Blood has the low viscosity of the continuous phase, the high concentration of the suspensions, and finally, the relative large size of RBCs and its aggregates compared to usual wall roughness. Therefore, significant amount of slip is to be expected for blood under the appropriate conditions. Slipping of RBCs in contact with the wall in vivo and in vitro has been observed in literature (Nubar, 1971). As a result of the shear induced migration of blood cells away from wall boundaries, a cell-rich layer surrounded by a cell-deplated plasma layer at the wall occurs (Phillips *et al.*, 1992). The interface between these layers is a rough surface due to the presence of the RBCs, and the protrusion of blood cells into the plasma layer may give additional energy dissipation (Sharan and Popel, 2001). Narrow marginal layer of plasma has a lower viscosity than the rest of the fluid and serve as a lubricant so that slip occurs. This can cause to an apparent decrease in the shear stress measured with rheometer or viscometer. In practice, in order to mitigate effect of slip, a vane type rheometer, a large enough viscometer gap size, roughening or profiling viscometer walls should be used (Barnes, 1995; Barnes, 2000). The slip effects and the effects of fibrinogen level and hematocrit on it at low shear rates were studied (Picart *et al.*, 1998a; Picart *et al.*, 1998b) and found that; migrational and slip effects are more pronounced as shear rate decreased, fibrinogen concentration is raised, and hematocrit is lowered. Aggregation behavior of RBCs at low shear rates and increase of the fibrinogen level could give rise to effective particle size, and lower hematocrit could give rise to the slip layer thickness. As a result, the slip effect can cause to experimental errors on viscosity data of whole blood if not eliminate or taken into account.

Another experimental limitation is that the viscosity models are based on experimental data obtaining the resulting shear stress response to shear rate after an acceptable amount of time has passed to allow rouleaux formation, although the time between consecutive strokes is not sufficiently long for the segregated RBC to reaggregate (O'Callaghan *et al.*, 2006).

3.2.1. Time independent viscosity models

All of non-Newtonian time-independent blood viscosity models show shear thinning behavior and must meet the following model requirements. There are three distinct regions for apparent blood viscosity; a lower Newtonian region (low shear rate constant viscosity, μ_o), an upper Newtonian region (high shear rate constant viscosity, μ_∞), and a middle region where the apparent viscosity is decreasing with increasing shear rate, $\partial\mu/\partial\gamma<0$. Power law equation is a suitable model for the middle region. However, it does not describe the low and high shear rate regions. Herschel-Bulkley model extends the power law model to include the yield stress, τ_y. The other models which include yield stress are also shown in Table 3. The models that have limitation at low and high shear rates can easily figure out when shear rate in models are taken as zero or infinity. Casson, Walburn-Schneck, and Weaver models include the effect of the RBC concentration, ε_{RBC}. Walburn-Schneck model also incorporates fibrinogen and globulins proteins, TPMA. A log-log plot of the apparent blood viscosity as a function of shear rate can be also used to figure out how much is closely matched each model and model parameters with healthy experimental blood viscosity data. The study on 11 viscosity models of Easthope and Brooks (1980) concluded that the Walburn and Schneck model is in well agreement in the shear rate range of 0.03-120 s^{-1}. Sugiura (1988) showed that viscosity model in that shear rate should be Weaver model. Wang and Stoltz (1994) deduced that K-L model provides the well description of hemorheological characteristic in the range of 0.2-180 s^{-1}. Zhang and Kuang (2000) found out that Bi-exponent, K-L and Quameda models can more precisely represent the hemorheological performance. Johnston *et al.* (2004) concluded that Ballyk model achieved a better approximation of WSS in low shear rate regions. O'Callaghan *et al.* (2006) showed that 9 viscosity models at high shear rates lead to similar WSS distribution while at lower shear rates they are qualitatively but not quantitatively similar. Case of study conditions (*e.g.*, the flow rate and geometry) must be also considered for determining the shear region under investigation, and then decided the appropriate viscosity model for own studies.

3.2.2. Time dependent viscosity models

Time-dependent models are used to describe thixotropic and viscoelastic behavior. Thixotropy is a special condition of pseudo plasticity with or without yield stress, where the apparent viscosity also decreases when the fluid is subjected to a constant shear rate. Blood is a concentrated suspension of cells. Most of concentrated suspension system exhibits thixotropic behavior. Experimental results of whole human blood have demonstrated that blood is a thixotropic fluid to be expected (Chen *et al.*, 1991; Huang *et al.*, 1987a; Huang *et al.*, 1987b; Thurston, 1979). The hematocrit, gender and age are factors affecting the blood thixotropy (Chen *et al.*, 1991; Huang *et al.*, 1987b). Huang developed a generalized rheological equation for thixo-

Table 3. Time independent non-Newtonian viscosity models

Power Law	$\mu = p(\dot{\gamma})^{n-1}$
p=14.67 mPas^n and n=0.7755 (Neofytou and Tsangaris, 2006), p=0.126, n=0.8004 units in cgs system (Buchanan *et al.*, 2000), p=9.267 mPas^n and n=0.828 (Kim *et al.*, 2000), and p=0.035 mPas^n and n=0.6 (Johnston *et al.*, 2004)	
Carreau Model	$\mu = \mu_\infty + (\mu_o + \mu_\infty)[1 + (\lambda\dot{\gamma})^2]^{(n-1)/2}$
λ=25 s, n=0.25, μ_o=0.025 poise, μ_∞=0.035 poise (Lee and Steinman, 2007), and λ=3.313 s, n=0.3568, μ_o=0.56 poise, μ_∞=0.0345 poise (Johnston *et al.*, 2004)	
Carreau-Yasuda Model	$\mu = \mu_\infty + (\mu_o + \mu_\infty)[1 + (\lambda\dot{\gamma})^{p_1}]^{(n-1)/p}$
λ=1.902 s, n=0.22, p=1.25, μ_o=0.56 poise and μ_∞=0.0345 poise (Cho and Kensey, 1991), λ=0.086 s, n=0.681, p=0.222, μ_o=12 mPas and μ_∞=1 mPas (Gijsen *et al.*, 1998), λ=0.438 s, n=0.191, p=0.409, μ_o=51.9 mPas and μ_∞=4.76 mPas (van de Vosse *et al.*, 2003), and λ=0.11 s, n=0.392, p=0.644, μ_o=22 mPas and μ_∞=2.2 mPas (Chen *et al.*, 2006)	
Ballyk Model	$\mu = \lambda(\dot{\gamma})(\dot{\gamma})^{n(\gamma)-1}$ where $\lambda(\dot{\gamma}) = \mu_\infty + \Delta\mu\exp[-(1+\lvert\dot{\gamma}\rvert/p_1)\exp(-p_2/\lvert\dot{\gamma}\rvert)]$ $n(\dot{\gamma}) = n_\infty + \Delta n\exp[-(1+\lvert\dot{\gamma}\rvert/p_3)\exp(-p_4/\lvert\dot{\gamma}\rvert)]$
μ_∞=0.0345, n_∞=1, $\Delta\mu$=0.25, Δn=0.45, p_1=50, p_2=3, p_3=50 and p_4=4 (Johnston *et al.*, 2004), and μ_∞=0.035 poise, n_∞=1, $\Delta\mu$=0.25, Δn=0.45, p_1=35.36, p_2=2.12, p_3=35.36 and p_4=2.83 (Lee and Steinman, 2007)	
Casson Model	$\mu = [(\eta^2 J_2)^{1/4} + 2^{-1/2}\tau_y^{1/2}]^2 J_2^{-1/2}$
$\lvert\dot{\gamma}\rvert = 2\sqrt{J_2}$, τ_y=0.1(0.625ε_{RBC})^3, $\eta=\mu_o(1-\varepsilon_{RBC})^{-2.5}$, μ_o=0.012 poise and ε_{RBC}=0.37 (Fung, 1993)	
The Herschel Bulkley Model	$\mu = p(\dot{\gamma})^{n-1} + (\tau_y/\dot{\gamma})$
p=8.9721 mPa·s^n, n=0.8601, τ_y=0.0175 N/m^2 (Valencia *et al.*, 2006)	
Walburn-Schneck Model	$\mu = p_1 e^{p_2\varepsilon_{RBC}}\left[e^{p_4(TPMA/\varepsilon_{RBC}^2)}\right](\dot{\gamma})^{-p_3\varepsilon_{RBC}}$
p_1=0.00797, p_2=0.0608, p_3=0.00499 p_4=14.585 1 g^{-1}, ε_{RBC}=40% and TPMA=25.9 g l^{-1} (Johnston *et al.*, 2004)	
Powell-Eyring Model	$\mu = \mu_\infty + (\mu_o - \mu_\infty)(\mathrm{Sinh}^{-1}\lambda\dot{\gamma})/(\lambda\dot{\gamma})$
λ=5.383 s, μ_o=0.56 poise and μ_∞=0.0345 poise (Cho and Kensey, 1991)	
Modified Powell-Eyring Model	$\mu = \mu_\infty + (\mu_o - \mu_\infty)\ln(\lambda\dot{\gamma}+1)/[\lambda\dot{\gamma}]^n$
λ=2.415 s, n=1.089, μ_o=0.56 poise and μ_∞=0.0345 poise (Cho and Kensey, 1991)	
Cross Model	$\mu = \mu_\infty + (\mu_o - \mu_\infty)/(1+(\lambda\dot{\gamma})^n)$
λ=1.007 s, n=1.028, μ_o=0.56 poise and μ_∞=0.0345 poise (Cho and Kensey, 1991)	
Simplified Cross Model	$\mu = \mu_\infty + (\mu_o - \mu_\infty)/(1+\lambda\dot{\gamma})$
λ=8.0 s, μ_o=1.3 poise and μ_∞=0.05 poise (Cho and Kensey, 1991)	
Modified Cross Model	$\mu = \mu_\infty + (\mu_o - \mu_\infty)/[1+(\lambda\dot{\gamma})^n]^p$
λ=8.2 s, n=0.64, p=1.23, μ_o=0.16 Pas and μ_∞=0.0035 Pas (Abraham *et al.*, 2005), and λ=3.736 s, n=2.406, p=0.254, μ_o=0.56 and μ_∞=0.0345 poise (Cho and Kensey, 1991)	
Quemada Model	$\mu = (\sqrt{\mu_\infty} + ((\sqrt{\tau_y})/(\sqrt{\lambda}+\sqrt{\dot{\gamma}})))$
μ_∞=0.02982 dyn s/cm^2, τ_y=0.2876 dyn/cm^2, λ=4.02 s^{-1} (Buchanan *et al.*, 2003), and μ_∞=0.02654, τ_y=0.04360, λ=0.02181 units in cgs system (Buchanan *et al.*, 2000)	

Table 3. Continued

K-L Model	$\tau = \tau_y + \mu_p(p_1\dot{\gamma} + p_2\sqrt{\dot{\gamma}})$
Wang Model	$\tau = \mu_p(p_1\dot{\gamma} + p_2\sqrt{\dot{\gamma}})$
Weaver Model	$\log\mu = \log\mu_p + (0.03 - 0.0076\log\gamma)\varepsilon_{RBC}$
Bi-Exponent Model	$\mu = p_1 + p_2\exp(-\sqrt{p_3\gamma}) + p_4\exp(-\sqrt{p_5\gamma})$
Ellis Model	$\tau = \dot{\gamma}/[(1/\mu_o) + p\tau^{(1/n)-1}]$
Sisko Model	$\mu = (\mu_\infty + p\dot{\gamma}^{n-1})$
Mizrahi-Berk Model	$\tau^{0.5} - \tau_y^{0.5} = p\dot{\gamma}^n$
Ofoli Model	$\tau^{n_1} = \tau_y^{n_1} + \mu_\infty(\dot{\gamma})^{n_2}$
Vocadlo Model	$\tau = [(\tau_y)^{1/n} + p\dot{\gamma}]^n$
Power Series Model	$\dot{\gamma} = p_1\tau + p_2(\tau)^3 + p_3(\tau)^5 + \ldots$
Van Wazer Model	$\mu = (\mu_o - \mu_\infty)/(1 + p_1\gamma + p_2(\dot{\gamma})^n) + \mu_\infty$
Reiner-Philippoff Model	$\tau = (\mu_\infty + (\mu_o - \mu_\infty)/(1 + ((\tau)^2/p)))\dot{\gamma}$
Heinz-Casson Model	$\tau^n = \tau_y^n + k\dot{\gamma}^n$
Robertson-Stiff Model	$\tau = p_1(p_2 + \dot{\gamma})^n$
Vinogradov-Malkin Model	$\mu = \mu_o/(1 + p_1\dot{\gamma}^n + p_2\dot{\gamma}^{2n})$
Kreiger Model	$\mu = \mu_\infty + (\mu_o - \mu_\infty)/(1 + p^n)$
Prandtl-Eyring Model	$\mu = \mu_\infty(\sinh^{-1}(\lambda\dot{\gamma})/(\lambda\dot{\gamma}))$
Hyperbolic Tangent Model	$\mu = \mu_\infty + (\mu_o - \mu_\infty)\tanh(\lambda\dot{\gamma})^n$

Table 4. Time dependent thixotropic models

Huang Model	$\tau - \tau_y = \mu\dot{\gamma} + CA\dot{\gamma}^m\exp(-C\int_0^t \dot{\gamma}^m dt)$	(Huang *et al.*, 1987a)
Weltman Model	$\tau = A_t - p\log t$	(Rao, 1999)
Tiu-Boger Model	$\tau = \varphi\tau_y + \varphi p(\dot{\gamma})^n$ $\frac{d\varphi}{dt} = -p_1(\varphi - \varphi_e)^2$	(Rao, 1999)
Rosen Model	$\mu = p(\dot{\gamma})^{n_1}(t)^{n_2}$	(Braun and Rosen, 2000)

tropic fluids. Huang model parameters were calculated from experimental data by non-linear parameter estimation technique for apparently healthy human subjects (Huang *et al.*, 1987a). Some thixotropic models are given in Table 4.

In literature, viscous models obtained at steady state conditions were used under pulsatile flow conditions. These models have provided a great deal of insight into the non-Newtonian viscous behavior of blood. However, blood exhibits both viscous and elastic properties under pulsatile flow (Thurston, 1972; Thurston, 1979). Viscosity is an assessment of the rate of energy dissipation due to cell deformation and sliding, while elasticity is an assessment of the elastic storage of energy primarily due to kinetic deformability of the RBCs (Thurston *et al.*, 2004). There are two dimensionless numbers to measure of the tendency of a material to appear either viscous or elastic; the Deborah number and the Weissenberg number. The Deborah number is the ratio of the relaxation time to the characteristic time of the flow.

$$De = \theta_r/T_c \quad (2)$$

The relaxation time can be defined as a ratio of the vis-

cosity to the elasticity;

$$\theta_r = \mu/G \tag{3}$$

Three ranges of Deborah number are identified as that; if $De \ll 1$, the material is viscous, if $De \sim 1$, the material will act viscoelastically, and if $De \gg 1$, the material is elastic (Steffe, 1996). The Weissenberg number is defined as the ratio of the characteristic time of fluid to a characteristic convective time-scale of the flow or the characteristic shear rate times the relaxation time.

$$We = \theta_r \dot{\gamma}_c \tag{4}$$

If the values of De and We are above a critical value, usually in the order of one, the elastic properties of the blood have to be taken into account (Gijsen *et al.*, 1999). The most appropriate choice of relaxation time of the RBCs is 0.06 s and the characteristic time of the flow is equal to the period time of the physiological flow pulse (Gijsen *et al.*, 1999).

Blood is slightly viscoelastic, and its effect was ignored in most of the CFD studies. At low shear rates, RBCs aggregate are solid-like bodies, and has ability to store elastic energy. Its value remains constant for shear rates up to 1 s^{-1} (Thurston, 1979). At high shear rates, its effect is less prominent because the RBCs behave fluid-like bodies (Schmid-Schönbein and Wells, 1969), and lose this ability (Anand and Rajagopal, 2004). Viscoelastic models can be suitable for blood flow under certain flow conditions especially at low shear stress. It also grows in importance when flow is oscillatory (Rojas, 2007). The extra stress tensor is used to characterize the viscoelastic stress in viscoelastic models. The total stress tensor (Cauchy stress tensor) is defined in terms of the pressure (P) and the extra stress tensor (S).

$$\sigma = -PI + S \tag{5}$$

Some of the extra stress tensors of these models are given below. There are common definitions in the models.

$$D = 0.5(L + L^T) \tag{6}$$

The symbol $(\overset{\nabla}{\cdot})$ denotes the upper convected derivative.

$$\overset{\nabla}{A} = \frac{\partial A}{\partial t} + \upsilon \cdot \nabla A - (\nabla \upsilon)^T \cdot A - A(\nabla \upsilon) \tag{7}$$

(i) Oldroyd-B Model:

$$S + \Lambda_1 \overset{\nabla}{S} = \mu(D + \Lambda_2 \overset{\nabla}{D}) \tag{8}$$

(ii) Yeleswarapu Model (Yeleswarapu *et al.*, 1998):

$$S + \Lambda_1[S - LS - SL^T] = \mu(A_1)[A_1] + \Lambda_2[A_1 - LA_1 - A_1L^T] \tag{9}$$

$$\mu(A_1) = \mu_\infty + (\mu_0 - \mu_\infty)\left[\frac{1 + \ln(1 + \eta\dot{\gamma})}{(1 + \eta\dot{\gamma})}\right] \tag{10}$$

$$\dot{\gamma} = \left[\frac{1}{2}\mathrm{tr}(A_1^2)\right]^{\frac{1}{2}} \tag{11}$$

where $A_1 = L + L^T$ is the first Rivlin-Ericksen Tensor, the dot indicates the material derivative. This model is a generalized Oldroyd-B model.

(iii) Generalized Oldroyd-B Model (Rajagopal and Srinivasa, 2000):

$$S = p_E B_{K_{p(t)}} + p_\mu D \tag{12}$$

$$S + \frac{p_\mu}{2p_E}\overset{\nabla}{S} = \eta_1\left(D + \frac{p_\mu}{2p_E}\overset{\nabla}{D}\right) + p_E\psi I \tag{13}$$

$$\psi = 3/\mathrm{tr}(B^{-1}_{K_{p(t)}}) \tag{14}$$

(iv) Generalized Maxwell Model (Rajagopal and Srinivasa, 2000):

$$S = p_E B_{K_{p(t)}} \tag{15}$$

$$\overset{\nabla}{B}_{K_{p(t)}} = -2\frac{p_E}{p_\mu}(B_{K_{p(t)}} - \psi I) \tag{16}$$

(v) Generalized Oldroyd-B Model (Anand and Rajagopal, 2004):

$$S = p_E B_{K_{p(t)}} + p_\mu D \tag{17}$$

$$\overset{\nabla}{B}_{K_{p(t)}} = -2\left(\frac{p_E}{p}\right)^{1+2n}(\mathrm{tr}(B_{K_{p(t)}}) - 3\lambda)^n[B_{K_{p(t)}} - \psi I] \tag{18}$$

$$n = (\gamma - 1)/(1 - 2\gamma);\ n > 0 \tag{19}$$

All of the Rajagopal models have a thermodynamic basis and generalized Oldroyd-B models of Rajogopal are not capable of an instantaneous elastic response.

(vi) Generalized Maxwell Model (Owens, 2006):

This model is based on homogenous flow assumption and derived from a simple structure dependent generalized Maxwell type constitutive equation for the elastic stress and identified the average aggregation size as a suitable structure variable.

$$S = \mu_p D + S_{elastic} \tag{20}$$

where $S_{elastic}$ represents the contribution to the extra stress due to the erythrocytes.

$$S_{elastic} + \Lambda_1(\dot{S}_{elastic} - \nabla\upsilon \cdot S_{elastic} - S_{elastic} \cdot \nabla\upsilon^T) = N_o k_B T_a \Lambda_1 D \tag{21}$$

$$\Lambda_1 = n_{ag}\Lambda_H/(1 + g_n n_{ag}\Lambda) \tag{22}$$

$$\frac{\partial n_{ag}}{\partial t} = -\frac{1}{2}b(\dot{\gamma})(n_{ag} - n_{st})(n_{ag} + n_{st} - 1) \tag{23}$$

$$n_{st} = \frac{\mu_o}{\mu_\infty}\left(\frac{1 + p_1\dot{\gamma}^n}{1 + p_2\dot{\gamma}^n}\right)\left(1 + \frac{3}{2}a(\dot{\gamma})N_o\Lambda_H\right) \tag{24}$$

$$b(\dot{\gamma}) = a(\dot{\gamma})N_o/(n_{st}(n_{st} - 1)) \tag{25}$$

Huang model is useful at a specific range of 0.1-10 s^{-1} (the range of blood thixotropy). Yeleswarapu model has the relaxation times, independent of shear rate as a limitation. Anand and Rajagopal (2004) determined that the best fit

with experimental data for both steady and oscillatory flow is obtained with their model than Yeleswarapu and generalized Oldroyd-B models. Owens model neglect the difference between the RBC number densities across the cross section.

3.3. Yield stress of blood

The yield stress of blood can be taken into account in the regions of low shear rates like thixotropic and viscoelastic behavior of blood. It can supply better understanding of aggregation and deformation of blood cells. The relation of cell deformation and aggregation with yield stress was described as (Zydney *et al.*, 1991);

$$\tau_y = \tau_{aggregation} + f \cdot \tau_{deformation} \quad (26)$$

where f is a coefficient (independent of shear rate and hemotocrit) characterizing the relative contributions of these two properties. All of data in Zydney's study were obtained with stored blood. However, they were in relatively good agreement with the data obtained by fresh whole blood and suspensions of fresh RBCs. The effect of cell aggregation was described as

$$\tau_{aggregation} = A_{aggregation}(\varepsilon_{RBC} - 0.05)^3, \quad \varepsilon_{RBC} \geq 0.05 \quad (27)$$

$$\tau_{aggregation} = 0, \quad \varepsilon_{RBC} < 0.05 \quad (28)$$

where $A_{aggregation}$ is a coefficient (71 ± 2 mPa). The effect of cell deformation was assumed to be of the form;

$$\tau_{deformation} = A_{deformation}(\varepsilon_{RBC} - 0.35)^3, \quad \varepsilon_{RBC} \geq 0.35 \quad (29)$$

$$\tau_{deformation} = 0, \quad \varepsilon_{RBC} < 0.35 \quad (30)$$

The experimental data fitted f with a deviation range of 0 ± 0.06. This showed insignificant effect of deformation on yield stress, and aggregation effect alone provided an accurate description of yield stress. Its dependence for 0.53 to 0.95 hemotocrit ranges is given in (Picart *et al.*, 1998a);

$$\tau_y = 26.87 \cdot \varepsilon_{RBC}^3 \quad (31)$$

There is no yield stress below a critical hemotocrit value (1-5%) (Merrill *et al.*, 1963) and the yield stress is (Luo and Kuang, 1992);

$$\tau_y = 0, \quad \varepsilon_{RBC} < \varepsilon_{critical} \quad (32)$$

$$\tau_y = 0.08(\varepsilon_{RBC} - \varepsilon_{critical})^3, \quad \varepsilon_{RBC} \geq \varepsilon_{critical} \quad (33)$$

where $\varepsilon_{critical}$ is critical hematocrit in the range of 5-8% (Luo and Kuang, 1992) and the unit of τ_y is yield stress in pascal. The yield stress as a function of hematocrit and fibrinogen concentration is given by (Arjomandi *et al.*, 2003);

$$\sqrt{\tau_y} = (\varepsilon_{RBC} - 0.1)(C_f + 0.5) \quad (34)$$

and with a coefficient of determination (r^2) 0.87 (Morris *et al.*, 1989);

$$\sqrt{\tau_y} = -0.091 + 0.47 \cdot \varepsilon_{RBC} + 0.22 \cdot C_f - 0.14 \cdot C_f^2 + 0.48 \cdot \varepsilon_{RBC} \cdot C_f \quad (35)$$

The yield stress of aggregated RBC suspensions is given as (Snabre and Mills, 1996);

$$\tau_y = \tau^* \left(\frac{\varepsilon_o^*}{\varepsilon_{RBC}} - 1 \right)^{-2} \quad \text{for } \varepsilon > \varepsilon_g \quad (36)$$

Accurately and functionally representing of blood behaviors in the viscosity models and the local hemodynamic environment are very important and increases performance of a CFD model. Therefore, there is a need for a viscosity model based on the internal structures of blood. Additionally, there are some cautions in the evaluation of accurate experimental data for blood constitutive parameters. The local environment strongly impacts the local flow patterns and hence shear rate. Expressing of accurate environment is therefore possibly essential. However, assumptions on the physiological conditions are mandatory.

4. Physiological conditions

The cyclic nature of the heart pump creates pulsatile conditions in arteries, and therefore blood flow and pressure are unsteady. The pulsations of flow are damped in the small vessels, and the flow is so effectively steady in the capillaries and the veins. The arteries are not rigid tubes. It adapts to varying flow and pressure conditions by enlarging or shrinking. All of these physiologic conditions and others cause difficulties to render simulations both conceptually and computationally tractable. As a result, most CFD models of arterial hemodynamics need to make the simplifying assumptions of rigid walls, steady flow, fully developed inlet velocities, Newtonian rheology, normal and periodic flow conditions, ignoring of small side or terminal branches, using of idealized or averaged artery models, and using of in vitro experiments to validate CFD models (Steinman, 2002; Steinman, 2004; Steinman and Taylor, 2005). No vessel movement resulting from organ movement such as coronary arteries movement resulting from heartbeat is also possible to add these assumptions. The advantages, limitation and accuracy of the medical imaging systems used for the construction of 3D vessel geometry model were also pinned down by Steinman (2002, 2004), and Steinman and Taylor (2005).

5. Conclusion

In this paper, the physical nature of human blood and its viscosity models have reasonably well documented. As referred previously in the body of the paper, some existing gaps can be identified as the challenging areas for future research.

1. Although there has been the considerable amount of viscosity models in blood rheology, none of them has

been commonly agreed upon or used. None of the models is fully expressing the effects of extremely complicated nature of blood rheology and its dependence of many factors. The groovy method used for obtaining the existing viscosity models is the parametric curve fitting on experimental apparent viscosity versus shear rate data, although the blood constitutive parameters in these models have been found to be related to internal structures of the blood such as RBC aggregation, RBC deformability, *etc.* The dependency of blood viscosity on each rheological property of the blood should be investigated and clarified separately by means of isolating the effects of remaining rheological properties.

2. The re-aggregation and viscoelastic behavior of blood detected in realistic pulsatile flows are much different from the corresponding behavior in steady flow. The blood viscosity models fitted on the data measured in the rheometer under the steady flow conditions are so not suitable for the analysis of realistic pulsatile blood flow. Observed blood apparent viscosity in the rheometers under the assumption of Newtonian flow pattern is also not suitable and the hematocrit value of tested blood also affects this pattern. The assumption of Newtonian pattern and neglecting the hematocrit effect on it can cause errors. The slip effect in the rheometers should also be prevented throughout the measurements.
3. Although there is a large number of studies on both Newtonian and non-Newtonian blood viscosity models in literature, there have been a variation on the critical value of limiting shear rate used for addressing the transition from non-Newtonian to Newtonian viscosity character of blood. Hematocrit dependence of this limiting shear rate value should be investigated for evaluating the proper application of both non-Newtonian to Newtonian viscosity models in CFD studies on blood flow.
4. Thixotropy must be considered in the regions of a substantial RBC residual time to allow the separated RBC to re-aggregate such as aneurysms and recirculation zones.
5. Viscoelasticity and thixotropy have generally accepted as less important for high shear regions. Even so, there is more need to develop in this area for low shear regions. Recent increases in study on viscoelastic models and its application in literature may be an evidence of this.
6. Making of a number of simplifying assumptions on physiologic conditions reduce very complicated construction of the realistic blood problem to a tractable problem to solve. However, each assumption grows away from realistic solution.

Acknowledgements

This study was financially supported by the Research Fund of the University of Gaziantep in terms of a research project coded as MF.07.06.

List of Symbols

A	the equilibrium value of structural parameter which indicates the relative amount of rouleaux in blood
A_1	the first Rivlin-Ericksen Tensor
A_t	the value of stress at t=1s
$a(\dot{\gamma})$	the aggregation rate
$B_{K_{p(t)}}$	the left Cauchy-Green elastic stretch tensor
$b(\dot{\gamma})$	the disaggregation rate
C	the kinetic rate constant of the structural breakdown of rouleaux into individual erythrocytes induced by shearing
C_f	fibrinogen concentration of plasma in grams per deciliter
D	the rate of deformation tensor
De	Deborah number
G	the elasticity
g_n	the average aggregate destruction rate coefficient
I	the unit tensor
K_η	the flux coefficients caused by gradients in the viscosity
K_c	the flux coefficients caused by gradients in the volume fraction
k_b	Boltzmann's constant
L	velocity gradient
N_o	number of red blood cells per unit volume
n_i	the empirical power constants(n_i=n, $n_{1,2,..}$)
m	the order of the structural breakdown reaction
n_{ag}	the average aggregate size
n_{st}	the steady state value of n_{ag} at a given shear rate
P	the isotropic pressure
p_i	the parameters of models(p_i=p, $p_{1,2,..}$)
p_μ	parameter relating viscosity
p_E	parameter relating elastic shear modules
$\bar{r}$	the ratio of the distance from tube axis to the radius of the tube
S	the extra stress tensor
$S_{elastic}$	the contribution to the extra stress due to the erythrocytes
T	temperature
T_a	absolute temperature
TPMA	the total plasma minus albumin
t	the time
We	Weissenberg number

Greek Symbols

$\dot{\gamma}$	the shear rate
$\dot{\gamma}_c$	the characteristic shear rate
ε	the volumetric concentration
ε_g	percolation threshold
ε_{max}	the maximum volume concentration
ε_{RBC}	the concentration of red blood cells
ε_w	the dispersed phase concentration at the tube wall
ε_o^*	the maximum packing volume fraction around the zero shear rate limit
$\varepsilon_{\eta_r=100}$	the dispersed phase concentration at which the relative viscosity becomes 100
η	the apparent viscosity
$[\eta]$	the intrinsic viscosity
θ_r	the relaxation time
κ	the correction factor
Λ_1	the relaxation times
Λ_2	the retardation times
Λ_H	the Maxwell relaxation time for a single red blood cell
λ	the time constant
μ	viscosity
μ_c	continuous phase viscosity
μ_d	dispersed phase viscosity
μ_p	the plasma viscosity
μ_r	the relative viscosity
μ_o	the low shear rate viscosity
μ_∞	the high shear rate viscosity
υ	the velocity
σ	the Cauchy stress tensor
τ	the shear stress
τ_y	the yield stress
τ^*	a characteristic shear stress for cluster break-up
φ	a time-dependent structural parameter
φ_e	an equilibrium value of the time-dependent structural parameter

References

Abraham, F., M. Behr and M. Heinkenschloss, 2005, Shape optimization in unsteady blood flow: a numerical study of non-Newtonian effects, *Comput. Meth. Biomech. Biomed. Eng.* **8**, 201-212.

Ai, L. and K. Vafai, 2005, An investigation of Stokes' second problem for non-Newtonian fluids, *Numer. Heat Tran. A* **47**, 955-980.

Anand, M. and K. R. Rajagopal, 2004, A shear-thinning viscoelastic fluid model for describing the flow of blood, *Int. J. Cardiovasc. Med. Sci.* **4**, 59-68.

Arjomandi, H., S. S. Barcelona, S. L. Gallocher and M. Vallejo, 2003, Biofluid dynamics of the human circulatory system, Proceedings of the congress on: "biofluid dynamics of the human body systems". Biomedical engineering institute, Florida international university, Miami - Florida, USA.

Bagchi, P., 2007, Mesoscale simulation of blood flow in small vessels, *Biophys. J.* **92** 1858-1877.

Bagchi, P., P. C. Johnson and A. S. Popel, 2005, Computational fluid dynamic simulation of aggregation of deformable cells in a shear flow, *J. Biomech. Eng.* **127**, 1070-1080.

Ballyk, P. D., D. A. Steinman and C. R. Ethier, 1994, Simulation of non-Newtonian blood flow in an end-to-side anastomosis, *Biorheology* **31**, 565-586.

Barnes, H. A., 1995, A review of the slip (wall depletion) of polymer solutions, emulsions and particle suspensions in viscometers: its cause, character, and cure, *J. of Non-Newtonian Fluid Mech.* **56**, 221-251.

Barnes, H. A., 2000, Measuring the viscosity of large-particle (and flocculated) suspensions - a note on the necessary gap size of rotational viscometers, *J. of Non-Newtonian Fluid Mech.* **94**, 213-217.

Barnes, H. A., J. F. Hutton and K. Walters, 1989, An introduction to rheology, Elsevier, Amsterdam.

Baskurt, O. K. and H. J. Meiselman, 1977, Cellular determinants of low-shear blood viscosity, *Biorheology* **34**, 235-247.

Baskurt, O. K. and H. J. Meiselman, 2003, Blood rheology and hemodynamics, *Semin. Thromb. Hemost.* **29**, 435-450.

Batchelor, G. K., 1977, The effect of Brownian motion on the bulk stress in a suspension of spherical particles, *J. Fluid Mech.* **83**, 97–117.

Baumler, H., B. Neu, E. Donath and H. Kiesewetter, 1999, Basic phenomena of red blood cell rouleaux formation biorheology, *Biorheology* **36**, 439-442.

Bishop J. J., A. S. Popel, M. Intaglietta and P. C. Johnson, 2001, Rheological effects of red blood cell aggregation in the venous network: a review of recent studies, *Biorheology* **38**, 263-274.

Braun, D. B. and M. R. Rosen, 2000, Rheology modifiers handbook: practical use and application, Noyes publications.

Brinkman, H. C., 1952, The viscosity of concentrated suspensions and solutions, *J. Chem. Phys.* **20**, 571-572.

Bronzino, J. D., 2006, The biomedical engineering handbook, Third edition, CRC.

Broughton, G. and L. Squires, 1938, The viscosity of oil–water emulsions, *J. Phys. Chem.* **42**, 253-263.

Buchanan, J. R., C. Kleinstreuer and J. K. Comer, 2000, Rheological effects on pulsatile hemodynamics in a stenosed tube, *Comput. Fluid* **29**, 695-724.

Buchanan, J. R., C. Kleinstreuer, S. Hyun and G. A. Truskey, 2003, Hemodynamics simulation and identification of susceptible sites of atherosclerotic lesion formation in a model abdominal aorta, *J. Biomech.* **36**, 1185-1196.

Çarpinlioglu, M. O. and M. Y. Gundogdu, 2001, A critical review on pulsatile pipe flow studies directing towards future research topics, *Flow. Meas. Instrum.* **12**, 163-174.

Chan, W. Y., Y. Ding and J. Y. Tu, 2007, Modeling of non-Newtonian blood flow through a stenosed artery incorporating fluid-structure interaction, *ANZIAM Journal* **47**, C507-C523.

Chen, H. Q., G. H. Zhong, L. Li, X. Y. Wang, T. Zhou and Z. Y. Chen, 1991, Effects of gender and age on thixotropic prop-

erties of whole blood from healthy adult subjects, *Biorheology* **28**, 177-183.

Chen, J., X. Lu and W. Wang, 2006, Non-Newtonian effects of blood flow on hemodynamics in distal vascular graft anastomoses, *J. Biomech.* **39**, 1983-1995.

Chien, S., 1970, Shear dependence of effective cell volume as a determinant of blood viscosity, *Science* **168**, 977-978.

Chien, S., S. Usami, R. J. Dellenback and M. I. Gregersen, 1970, Shear-dependent interaction of plasma proteins with erythrocytes in blood rheology, *Am. J. Physiol.* **219**, 143-153.

Cho, Y. I. and K. R. Kensey, 1991, Effects of the non-Newtonian viscosity of blood on hemodynamics of diseased arterial flows: part 1, steady flows, *Biorheology* **28**, 241-262.

Chong, J. S., E. B. Christiansen and A. D. Baer, 1971, Rheology of concentrated suspension, *J. Appl. Polymer Sci.* **15**, 2007-2021.

Cosgrove, T., 2005, Colloid science: principles, methods and applications, Blackwell publishing limited.

Coussot, P., 2005, Rheometry of pastes, suspensions, and granular materials: applications in industry and environment, Wiley-Interscience.

Cristini, V. and G. S. Kassab, 2005, Computer modeling of red blood cell rheology in the microcirculation: a brief overview, *Ann. Biomed. Eng.* **33**, 1724-1727.

Crowley, T. A. and V. Pizziconi, 2005, Isolation of plasma from whole blood using planar microfilters for lab-on-a-chip applications, *Lab Chip* **5**, 922-929.

De Gruttola, S., K. Boomsma and D. Poulikakos, 2005, Computational simulation of a non-Newtonian model of the blood separation process, *Artif. Organs* **29**, 949-959.

Dintenfass, L., 1968, Internal viscosity of the red cell and a blood viscosity equation, *Nature* **219**, 956-958.

Dupin, M. M., I. Halliday, C. M. Careand, L. Alboul and L. L. Munn, 2007, Modeling the flow of dense suspensions of deformable particles in three dimensions, *Phys. Rev. E* **75**, 066707.

Easthope, P. and D. E. Brooks, 1980, A comparison of constitutive functions for whole human blood, *Biorheology* **17**, 235-247.

Eilers, H., 1941, Die viskosität von emulsionen hochviskoser stoffe als funktion der konzentration, *Kolloid-Z* **97**, 313-321.

Einstein, A., 1911, Berichtigung zu meiner arbeit: eine neue bestimmung der moleküldimensionen, *Ann. Phys.* **339**, 591-592.

Frankel N. A. and A. Acrivos, 1967, On the viscosity of a concentrated suspension of solid particles, *Chem. Eng. Sci.* **22**, 847-853.

Fung, Y. C. 1993 Biomechanics: mechanical properties of living tissues, 2nd ed. Springer-Verlag, New York.

Gijsen, F. J. H., F. N. van de Vosse and J. D. Janssen, 1998, Wall shear stress in backward-facing step flow of a red blood cell suspension, *Biorheology* **35**, 263-79.

Gijsen, F. J. H., E. Allanic, F. N. van de Vosse and J. D. Janssen, 1999, The influence of the non-Newtonian properties of blood on the flow in large arteries: unsteady flow in a 90-degree curved tube, *J. Biomech.* **32**, 705-713.

Gundogdu, M. Y. and M. O. Çarpinlioglu, 1999a, Present state of art on pulsatile flow theory, part 1. laminar and transitional flow regimes, *JSME Int. J.* **42**, 384-397.

Gundogdu, M. Y. and M. O. Çarpinlioglu, 1999b, Present state of art on pulsatile flow theory, part 2. turbulent flow regime, *JSME Int. J.* **42**, 398-410.

Hatschek, E., 1911, Die viskosität der dispersoide, *Kolloid-Z* **8**, 34-39.

Huang, C. R., W. D. Pan, H. Q. Chen and A. L. Copley, 1987a, Thixotropic properties of whole blood, *Biorheology* **24**, 795-801.

Huang, C. R., H. Q. Chen, W. D. Pan, T. Shih, D. S. Kristol and A. L. Copley, 1987b, Effects of hematocrit on thixotropic properties of human blood, *Biorheology* **24**, 803-810.

Janzen, J., T. G. Elliott, C. J. Carter and D. E. Brooks, 2000, Detection of red cell aggregation by low shear rate viscometry in whole blood with elevated plasma viscosity, *Biorheology* **37**, 225-237.

Jeffery, G. B., 1922, The motion of ellipsoidal particles immersed in a viscous fluid, *Proc. Roy. Soc. Lond. A* **102**, 161-179.

Johnston, B. M., P. R. Johnston, S. Corney and D. Kilpatrick, 2004, Non-Newtonian blood flow in human right coronary arteries: steady state simulations, *J. Biomech.* **37**, 709-720.

Joye, D. D., 2003, Shear rate and viscosity corrections for a Casson fluid in cylindrical (Couette) geometries, *J. Colloid Interface Sci.* **267**, 204-210.

Kang, I. S., 2002, A microscopic study on the rheological properties of human blood in the low concentration limit, *Korea Aust. Rheol. J.* **14**, 77-86.

Kim S., Y. I. Cho, A. H. Jeon, B. Hogenauer and K. R. Kensey, 2000, A new method for blood viscosity measurement, *J. Non-Newtonian Fluid Mech.* **94**, 47-56.

Kitano, T., T. Kataoka and T. Shirota, 1981, An empirical equation of the relative viscosity of polymer melts filled with various inorganic fillers, *Rheol. Acta* **20**, 207-209.

Krieger, I. M., 1972, Rheology of monodisperse lattices, *Adv. Colloid Interface Sci.* **3**, 111-136.

Krieger, I. M., and T. J. Dougherty, 1959, A mechanism for non-Newtonian flow in suspension of rigid spheres, *T. Soc. Rheol.* **3**, 137-152.

Lee, S. W. and D. A. Steinman, 2007, On the relative importance of rheology for image-based CFD models of the carotid bifurcation, *J. Biomech. Eng.* **129**, 273-278.

Leondes, C. T., 2000, Biomechanical systems: techniques and applications, volume IV: biofluid methods in vascular and pulmonary systems: techniques and applications: 4 CRC Press.

Lew, H. S., 1969, Formulation of statistical equation of motion of blood, *Biophys. J.* **9**, 235-245.

Liu, Y., L. Zhang, X. Wang and W. K. Liu, 2004, Coupling of Navier-Stokes equations with protein molecular dynamics and its application to hemodynamics, *Int. J. Numer. Meth. Fluid* **46**, 1237-1252.

Liu, Y. and W. K. Liu, 2006, Rheology of red blood cell aggregation by computer simulation, *J. Comput. Phys.* **220**, 139-154.

Long, D. S., M. L. Smith, A. R. Pries, K. Ley and E. R. Damiano, 2004, Microviscometry reveals reduced blood viscosity and altered shear rate and shear stres profiles in microvessels after hemodilution, *PNAS* **101**, 10060-10065.

Luo, X. Y. and Z. B. Kuang, 1992, A study on the constitutive equation of blood, *J. Biomech.* **25**, 929-934.

Malkin, A. Y., 1994, Rheology fundamentals, ChemTec Publishing.

Maron, S. H. and P. E. Pierce, 1956, Application of Ree-Eyring generalized flow theory to suspensions of spherical particles, *J. Colloid Interface Sci.* **11**, 80-95.

Mazumdar, J. N., 1998, Biofluid mechanics, World Scientific.

Meiselman, H. J. and O. K. Baskurt, 2006, Hemorheology and hemodynamics; dove andare?, *Clin. Hemorheol. Micro.* **35**, 37-43.

Merrill, E. W., G. C. Cokelet, A. Britten and R. E. Wells, 1963, Non-Newtonian rheology of human blood - effect of fibrinogen deduced by "subtraction", *Circ. Res.* **13**, 48-55.

Mooney, M. J., 1951, The viscosity of a concentrated suspension of spherical particles, *J. Colloid Interface Sci.* **6**, 162-170.

Morris, C. L., D. L. Rucknagel, R. Shukla, R. A. Gruppo, C. M. Smith and P. Blackshear, 1989, Evaluation of the yield stress of normal blood as a function of fibrinogen concentration and hematocrit, *Microvasc. Res.* **37**, 323-338.

Neofytou, P. and S. Tsangaris, 2006, Flow effects of blood constitutive equations in 3D models of vascular anomalies, *Int. J. Numer. Meth. Fluid* **51**, 489-510.

Nubar, Y., 1971, Blood flow, slip, and viscometry, *Biophys. J.* **11**, 252-264.

O'Callaghan, S., M. Walsh and T. McGloughlin, 2006, Numerical modelling of Newtonian and non-Newtonian representation of blood in a distal end-to-side vascular bypass graft anastomosis, *Med. Eng. Phys.* **28**, 70-74.

Owens, R. G., 2006, A new microstructure-based constitutive model for human blood, *J. Non-Newtonian Fluid Mech.* **140**, 57-70.

Pal, R., 2003, Rheology of concentrated suspensions of deformable elastic particles such as human erythrocytes, *J. Biomech.* **36**, 981-989.

Pal, R. and E. Rhodes, 1989, Viscosity/concentration relationships for emulsions, *J. Rheol.* **33**, 1021-1045.

Phillips, R. J., R. C. Armstrong, R. A. Brown, A. L. Graham and Abbott, J.R., 1992, A constitutive equation for concentrated suspensions that accounts for shear-induced particle migration, *Phys. Fluid.* **4**, 30-40.

Picart, C., J-M. Piau, H. Galliard and P. Carpentier, 1998a, Human blood shear yield stress and its hematocrit dependence, *J. Rheol.* **42**, 1-12.

Picart, C., J. M. Piau, H. Galliard and P. Carpentier, 1998b, Blood low shear rate rheometry: influence of fibrinogen level and hematocrit on slip and migrational effects, *Biorheology* **35**, 335-353.

Popel A. S., and P. C. Johnson, 2005, Microcirculation and hemorheology, *Annu. Rev. Fluid Mech.* **37**, 43-69.

Quemada, D., 1978, Rheology of concentrated disperse systems II. A model for non-Newtonian shear viscosity in steady flows, *Rheol. Acta* **17**, 632-642.

Rajagopal, K. R. and A. R. Srinivasa, 2000, A thermodynamic frame work for rate type fluid models, *J. Non-Newtonian Fluid Mech.* **88**, 207-227.

Rampling, M. W., H. J. Meiselman, B. Neub and O. K. Baskurt, 2004, Influence of cell-specific factors on red blood cell aggregation, *Biorheology* **41**, 91–112.

Rao, M. A., 1999, Rheology of fluids and semisolid foods: principles and applications, Springer - Verlag.

Richardson, E. G., 1933, Über die viskosität von emulsionen, *Kolloid-Z* **65**, 32-37.

Rojas, H. A. G., 2007, Numerical implementation of viscoelastic blood flow in a simplified arterial geometry, *Med. Eng. Phys.* **29**, 491-496.

Roscoe, R., 1952, The viscosity of suspensions of rigid spheres, *Br. J. Appl. Phys.* **3**, 267-269.

Rovedo, C. O., P. E. Viollaz and C. Suarez, 1991, The effect of pH and temperature on the rheological behavior of Dulce de leche, a typical dairy Argentine product, *J. Dairy Sci.* **74**, 1497-1502.

Schmid-Schönbein, H. and R. Wells, 1969, Fluid drop-like transition of erythrocytes under shear, *Science* **165**, 288-291.

Schramm, L. L., 2005, Emulsions, foams, and suspensions: fundamentals and applications, Wiley-VCH.

Sharan, M. and A. S. Popel, 2001, A two-phase model for flow of blood in narrow tubes with increased effective viscosity near the wall, *Biorheology* **38**, 415-428.

Sibree, J. O., 1931, The viscosity of emulsions: part II, *Trans. Faraday Soc.* **27**, 161-176.

Snabre, P. and P. Mills, 1996, II. Rheology of weakly flocculated suspensions of viscoelastic particles, *J. Phys. III* **6**, 1835-1855.

Steffe, J. F., 1996, Rheological methods in food process engineering, 2nd ed. Freeman Press.

Steinman, D. A., 2002, Image-based computational fluid dynamics modeling in realistic arterial geometries, *Ann. Biomed. Eng.* **30**, 483-497.

Steinman, D. A., 2004, Image-based computational fluid dynamics: a new paradigm for monitoring hemodynamics and atherosclerosis, *Curr. Drug Targets Cardiovasc. Haematol. Disord.* **4**, 183-197.

Steinman, D. A. and C. A. Taylor, 2005, Flow imaging and computing: large artery hemodynamics, *Ann. Biomed. Eng.* **33**, 1704-1709.

Sugiura, Y., 1988, A method for analyzing non Newtonian blood viscosity data in low shear rates, *Biorheology* **25**, 107-112.

Taylor, G. I., 1932, The viscosity of a fluid containing small drops of another fluid, *Proc. Roy. Soc. Lond. A* **138**, 41-48.

Thomas, D. G., 1965, Transport characteristics of suspension: VIII. A note on the viscosity of Newtonian suspensions of uniform spherical particles, *J. Colloid Interface Sci.* **20**, 267-277.

Thurston, G. B., 1972, Viscoelasticity of human blood, *Biophys. J.* **12**, 1205-1217.

Thurston, G. B., 1979, Rheological parameters for the viscosity, viscoelasticity, and thixotropy of blood, *Biorheology* **16**, 149-162.

Thurston, G. B., N. M. Henderson and M. Jeng, 2004, Effects of erythrocytapheresis transfusion on the viscoelasticity of sickle cell blood, *Clin. Hemorheol. Micro.* **30**, 61-75.

Thurston, G. B. and N. M. Henderson, 2006, Effects of flow geometry on blood viscoelasticity, *Biorheology* **43**, 729-746.

Toda, K. and H. Furuse, 2006, Extension of Einstein's viscosity equation to that for concentrated dispersions of solutes and

particles, *J. Biosci. Bioeng.* **102**, 524-528.

Valencia, A., A. Zarate, M. Galvez and L. Badilla, 2006, Non-Newtonian blood flow dynamics in a right internal carotid artery with a saccular aneurysm, *Int. J. Numer. Meth. Fluid* **50**, 751-764.

van de Vosse, F. N., J. de Hart, C. H. G. A. van Oijen, D. Bessems, T. W. M. Gunther, A. Segal, B. J. B. M. Wolters, J. M. A. Stijnen and F. P. T. Baaijens, 2003, Finite-element-based computational methods for cardiovascular fluid-structure interaction, *J. Eng. Math.* **47**, 335-368.

Vand, V., 1948, Viscosity of solutions and suspensions. 1. Theory, *J. Phys. Colloid Chem.* **52**, 277-299.

Vocadlo, J. J., 1976, Role of some parameters and effective variables in turbulent slurry flow, Proceedings of the hydro- transport 4 conference, BHRA, Cranfield, U.K., Paper D4, 49-62.

Wang, X., J. F. Stoltz, 1994, Characterization of pathological blood with a new rheological relationship, *Clin. Hemorheol.* **14**, 237-245.

Wildemuth, C. R. and M. C. Williams, 1984, Viscosity of suspensions modeled with a shear-dependent maximum packing fraction, *Rheol. Acta* **23**, 627-635.

Yeleswarapu, K. K., M. V. Kameneva, K. R. Rajagopal and J. F. Antaki, 1998, The flow of blood in tubes: theory and experiment, *Mech. Res. Comm.* **25**, 257-262.

Zhang, J., P. C. Johnson and A. S. Popel, 2007, An immersed boundary lattice Boltzmann approach to simulate deformable liquid capsules and its application to microscopic blood flows, *Phys. Biol.* **4**, 285-295.

Zhang, J., P. C. Johnson and A. S. Popel, 2008, Red blood cell aggregation and dissociation in shear flows simulated by lattice Boltzmann method, *J. Biomech.* **41**, 47-55.

Zhang, J .B. and Z. B. Kuang, 2000, Study on blood constitutive parameters in different blood constitutive equations, *J. Biomech.* **33**, 355-360.

Zydney, A. L., J. D. Oliver and C. K. Colton, 1991, A constitutive equation for the viscosity of stored red blood cell suspensions: effect of hematocrit, shear rate, and suspending phase, *J. Rheol.* **35**, 1639-1680.